



ChemComm

Zinc phthalocyanine - benzoperylenetriimide conjugate for solvent dependent ultrafast energy vs electron transfer

Journal:	<i>ChemComm</i>
Manuscript ID	CC-COM-09-2019-007649.R1
Article Type:	Communication

SCHOLARONE™
Manuscripts

Zinc phthalocyanine - benzoperylene triimide conjugate for solvent dependent ultrafast energy vs electron transfer[†]

Valeria Navarro-Pérez,^a Ana M. Gutiérrez-Vílchez,^a Javier Ortiz,^a Ángela Sastre-Santos,^a Fernando Fernández-Lázaro,^{*a} Sairaman Seetharaman,^b M. J. Duffy,^c Paul A. Karr,^c and Francis D'Souza^{*b}

Received (in XXX, XXX) Xth XXXXXXXXXX 200X, Accepted Xth XXXXXXXXXX 200X

First published on the web Xth XXXXXXXXXX 200X

DOI: 10.1039/b000000x

A novel zinc phthalocyanine - benzoperylene triimide conjugate has been synthesized and its ability to undergo ultrafast energy and electron transfer as a function of solvent polarity has been demonstrated using femtosecond transient absorption (fs-TA) technique operating at femto- to nanosecond time scale.

Photoinduced energy and/or electron transfer processes are the subject of an increasing number of studies as they are major events in naturally-occurring and artificial photosynthesis and also in solar cells.¹ The most common approach to synthetic systems displaying such processes relies in the covalent binding (molecular systems) or in the intermolecular bonding (supramolecular systems) of electron-rich moieties with electron-poor units. Among the former group, porphyrins and the structurally-related phthalocyanines have been widely used, based on the fact that the primary actor in the photosynthesis is indeed a porphyrin derivative. Phthalocyanines (Pcs), in particular, are extraordinary building blocks due to several features like their thermal and chemical resistance, their huge absorption in the red part of the visible spectrum, the possibility of modulation of their properties as a function of the central metal and the substituents in the peripheral and/or axial (metal permitting) positions, and their ability to act as electron donors or acceptors, among others.² Thus, several examples of Pc-electron acceptor systems have been studied.³

Perylenediimides (PDIs), on the other hand, are one of the most employed prototypes of electron-acceptor molecules due to their chemical persistency, their strong absorption in the visible region, their relatively high fluorescence quantum yields and the modulability of their properties depending on the substituents at the imide-bay-ortho positions.⁴ They have also been extensively used in the preparation of PDI-electron donor structures.⁵

Needless to say that Pcs and PDIs have been combined in a plethora of arrangements varying the number of subunits (dyads, triads, pentads...), the class of linkage (covalent, coordinative, hydrogen bonding) and its position (on the periphery or the central metal of the Pc, at the imide, bay or ortho positions of the PDI).⁶ The existence of low-lying triplet excited states of the Pc and, specially, of the PDI leads to short-lived charge separated (CS) states, typically in the range of the pico- or even nanoseconds. The addition of magnesium ions dramatically elongates the lifetime of the CS state as a

result of their complexation with the radical-anion of the PDI, thus stabilizing the CS state.⁷ However, the generation of a long-lived CS state in a Pc-PDI dyad is possible without the intermediacy of any metal ion by an appropriate selection of the substituents present in both subunits, which leads to a CS state lower in energy than the triplet excited states and to lifetimes in the hundreds of μ s domain.⁸

In this context, we decided to explore the ability of benzo[ghi]perylene triimides (BPTIs) to substitute PDIs as electron acceptors taking into account the presence of three electron deficient imide groups. These compounds were first described by Langhals,⁹ but have scarcely been conjugated with other electroactive moieties, such as corrole, tetrathiafulvalene, naphthalenediimide, PDI and itself.¹⁰ In this contribution we describe the synthesis, characterization and photophysical study of BPTI-ZnPc dyad **1**. The ZnPc and BPTI entities have complementary absorption and fluorescence properties making it a highly useful dyad for light energy harvesting applications. Photoinduced energy and electron transfer as a function of solvent polarity has been demonstrated mimicking early events of natural photosynthesis.

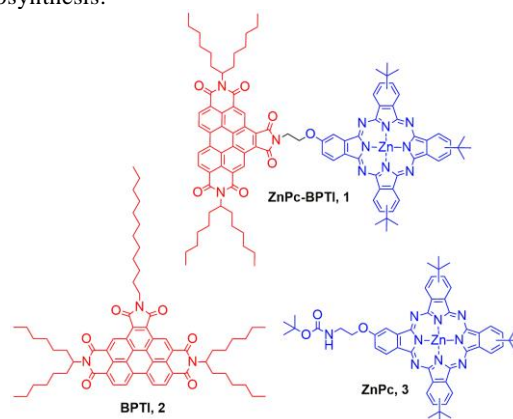


Chart 1 Chemical structures of dyad **1** and the control compounds **2** and **3**.

ZnPc-BPTI dyad **1** and reference BPTI **2** were synthesized by a condensation reaction between a benzoperylene diimide monoanhydride and an amino-substituted phthalocyanine or dodecylamine, respectively. For details on the procedures and characterization, see ESI. Reference ZnPc **3** was prepared according to the literature.¹¹ Newly synthesized compounds were fully characterized using ¹H and ¹³C NMR and Maldi-mass techniques.

Fig. 1a shows the absorption spectrum of dyad **1** along with

the control compounds. Subtle spectral changes were observed for the dyad compared to the spectrum of equimolar mixture of **2** and **3**. That is, 5-10 nm red-shift accompanied by broadening of BPTI and ZnPc peaks were observed. These results indicate intramolecular interactions between the two entities in the ground state. The fluorescence peaks of BPTI were located at 484, 514, and 553 nm that was not quenched (<5%) when the solution was mixed with equimolar ZnPc indicating absence of intermolecular interactions. However, in the dyad, the BPTI emission peak was quenched over 94% (Fig. 1b). Similar results were also observed when ZnPc entity in the dyad was excited (Fig. 1c). The ZnPc peak located at 690 nm was quenched over 98% in the dyad. These results indicate occurrence of intramolecular photochemical events originating from both $^1\text{BPTI}^*$ and $^1\text{ZnPc}^*$ excited states in the dyad. As shown in Fig. S9 in ESI, the fluorescence lifetimes measured using time correlated single photon counting (TCSPC) technique gave lifetimes for $^1\text{BPTI}^*$ or $^1\text{ZnPc}^*$, respectively, as 8.84 and 2.83 ns. However, in the case of the dyad, these lifetimes were within the lower detection limit of our TCSPC setup, meaning efficiently quenched $^1\text{BPTI}^*$ and $^1\text{ZnPc}^*$ excited states.

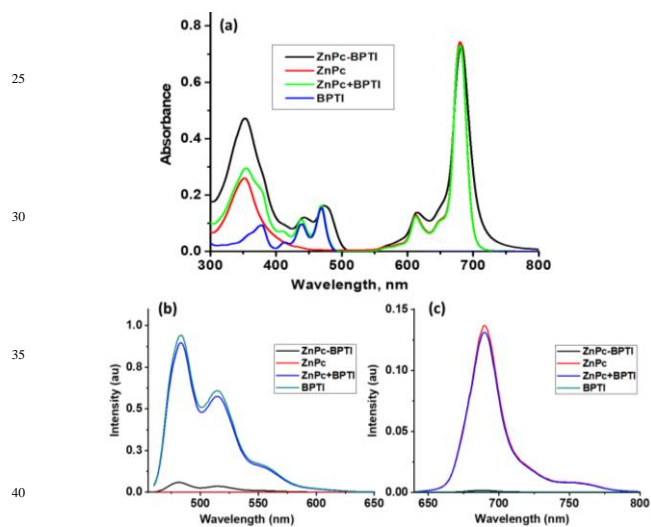


Fig. 1. (a) Absorption, (b) fluorescence spectrum exciting BPTI ($\lambda_{\text{exc}} = 440$ nm) and (c) exciting ZnPc ($\lambda_{\text{exc}} = 615$ nm) of the indicated compounds in benzonitrile.

Electrochemical and computational studies were subsequently performed to identify the donor and acceptor entities of the dyads (Fig. 2a). The first reversible oxidation and first two reversible reductions of ZnPc were located at 0.57, -0.95 and -1.10 V while the first two reversible reductions of BPTI were located at -0.53 and -0.85 V vs. Ag/AgCl (Fig. 2a). In the dyad, the ZnPc oxidation was located at 0.63 V while the reductions were located at -0.57, -0.83 (corresponding to BPTI) and -1.06 (ZnPc). The slightly anodic shift of ZnPc oxidation and cathodic shift of BPTI reductions suggest intramolecular interactions, as evidenced from absorption studies. Computational studies were performed at the B3LYP/6-311G(d,p) level using *Gaussian 16*¹² to help visualize the geometry and location of the frontier orbitals (Fig. 2b). In the optimized structure, the ZnPc and BPTI planes were perpendicular to one another with the zinc to the closest BPTI N distance of 11.46 Å. The HOMO was fully located on the ZnPc and LUMO was on the BPTI entity. The electron rich (blue) and poor (red) locations within the dyad could be visualized from the molecular electrostatic map

(MEP, Fig. 2b(iii)). From these studies, ZnPc as electron donor and BPTI as electron acceptor are borne out. The $\text{BPTI}^{\cdot-}$ from spectroelectrochemical studies is characterized by bands at 531, 644, 720 and 864 nm¹³ while ZnPc^+ is known for a near-IR peak at 840 nm.¹⁴

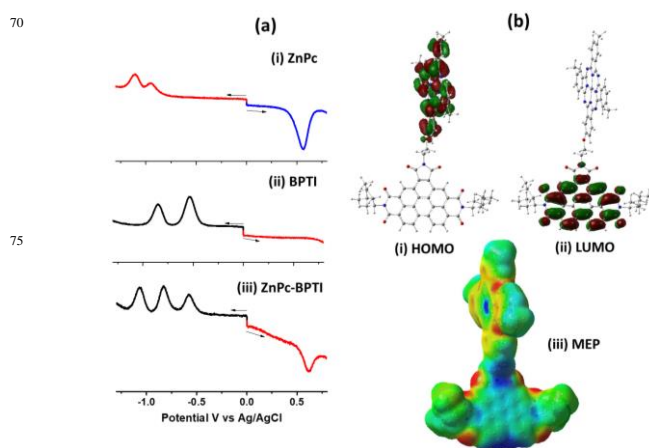


Fig. 2. (a) Differential pulse voltammograms of the indicated compounds in PhCN containing 0.1 M (TBA)ClO₄. (b) The HOMO, LUMO and MEP of the optimized dyad was visualized from GaussView program.

An energy level diagram visualizing the different photochemical events was established as shown in Fig. 3. For this scheme, energy of the singlet excited states, $^1\text{ZnPc}^*$ and $^1\text{BPTI}^*$, was calculated from the 0,0 transitions of absorption and fluorescence peak maxima of ZnPc and BPTI, energy of charge separated states was calculated from the optical, electrochemical and computational data using Rehm and Weller approach,¹⁵ and the energy of triplet excited state was taken from literature.¹⁶

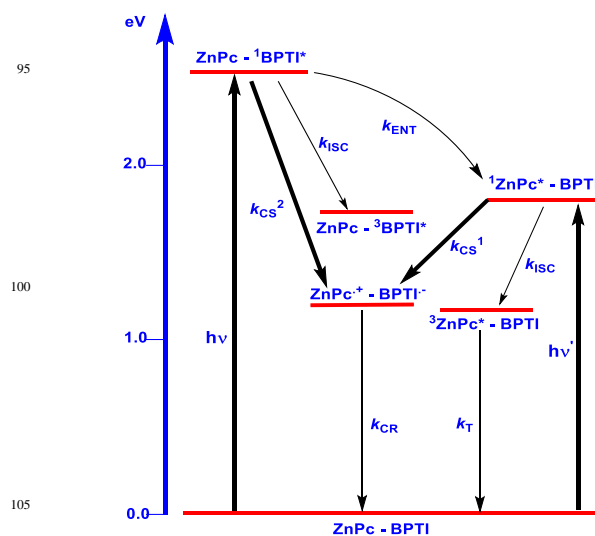


Fig. 3. Energy level diagram depicting different photochemical events in the ZnPc-BPTI dyad upon selective excitation of either ZnPc or BPTI entities. CS=charge separation, CR=charge recombination, T=triplet emission, ISC=intersystem crossing, k =rate constant, ENT=energy transfer. Thick and thin arrows represent major and minor processes, respectively.

A glance at the energy level diagram suggests the possibility of singlet excitation transfer from $^1\text{BPTI}^*$ to ZnPc,

electron transfer from both $^1\text{BPTI}^*$ and $^1\text{ZnPc}^*$ leading to $\text{ZnPc}^+-\text{BPTI}^-$ charge separated state, and location of the energy of the charge-separated state below that of $^3\text{BPTI}^*$ and $^3\text{ZnPc}^*$. Under such conditions, $\text{ZnPc}^+-\text{BPTI}^-$ could relax to the ground state directly. In order to verify the photochemical reaction mechanism and to evaluate the kinetic parameters, fs-TA studies in polar benzonitrile and nonpolar toluene were carried out by selectively exciting the BPTI and ZnPc entities of the dyad.

First, transient spectral features of the control ZnPc and BPTI were recorded as shown in Figure S10 in ESI. For ZnPc in toluene, the instantaneously formed $^1\text{ZnPc}^*$ revealed positive peaks at 594, 634, 819, and a broad signal at 1330 nm due to excited state absorption (ESA). Negative signals at 611, 682, and 752 nm having contributions from ground state bleach (GSB) and stimulated emission (SE) were also observed. The decay and recovery of the positive and negative peaks revealed a new peak at 510 nm corresponding to $^3\text{ZnPc}^*$ formed via intersystem crossing (ISC) process. For $^1\text{BPTI}^*$ in toluene, the ESA peaks were located at 682 and 718 nm while the GSB and SE peaks were in the 438 and 480 nm range. Decay and recovery of the transient signals resulted in new set of peaks at 500 and 532 nm due to the formation of $^3\text{BPTI}^*$.¹⁶ The transient signals corresponding to both $^1\text{ZnPc}^*$ and $^1\text{BPTI}^*$ lasted over 3 ns consistent with their long-lived fluorescence lifetimes. Similar spectral trends were also observed in benzonitrile.

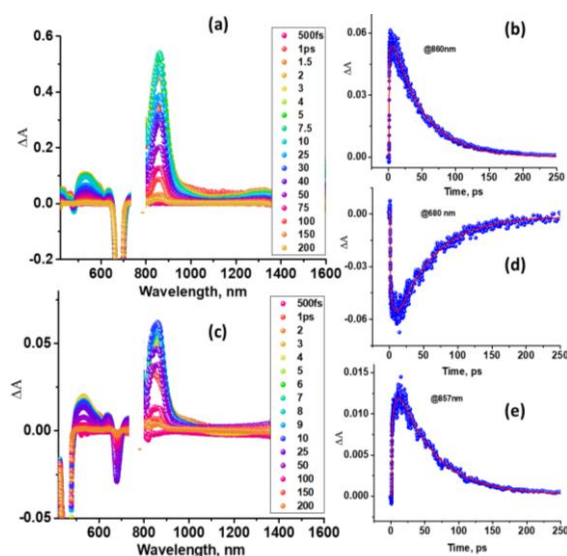


Fig. 4. Fs-TA at the indicated delay times of ZnPc-BPTI dyad in benzonitrile at the λ_{ex} of (a) 686 nm and (c) 466 nm. Time profile of 860 nm peak for the data shown in Fig. 4a is shown in b while that at 680 and 857 nm for the data shown in Fig. 4c are shown in d and e, respectively.

Fs-TA spectra at the indicated delay times of dyad in benzonitrile at donor and acceptor excitation wavelengths is shown in Fig. 4. At the excitation wavelength of 686 nm, ultrafast charge separation from the $^1\text{ZnPc}^*$ state was witnessed. Characteristic transient peaks in the 800-900 nm region comprised of both ZnPc^+ and BPTI^- were observed (Fig. 4a). From the rise and decay of the radical peaks, time constants for charge separation (CS) and charge recombination (CR) were found to be 4.34 and 47 ps (Fig. 4b). Interestingly, when the sample was excited at 466 nm, corresponding to BPTI, two photochemical events were

obvious. That is, growth of $^1\text{ZnPc}^*$ SE peak at 680 nm due to excitation transfer, and peaks corresponding to the charge separated state in the 800-900 nm region (Fig. 4c). The time profile for the former process shown in Fig. 4d revealed time constants of 16.7 (growth) and 50 ps (recovery) while that of the charge separated state were 5.8 (CS) and 55 ps (CR) (Fig. 4e). The closeness of these time constants suggest simultaneous occurrence of energy and electron transfer processes in this dyad.

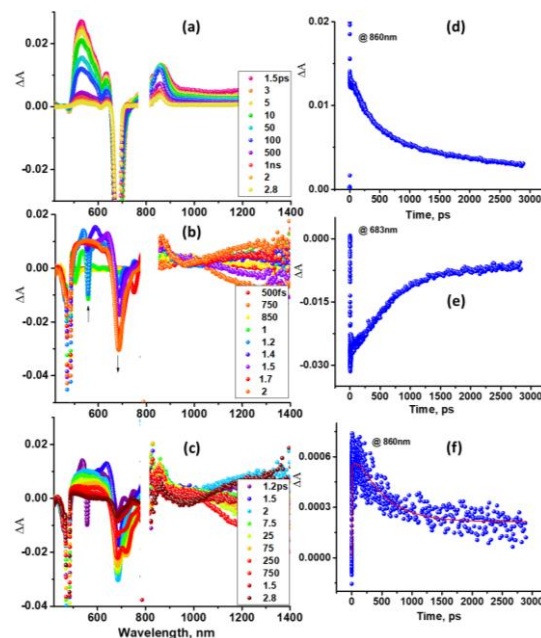


Fig. 5. Fs-TA spectra at the indicated delay times of ZnPc-BPTI at the λ_{ex} of (a) 686 nm, (b) and (c) at 466 nm in toluene. Time profile of (d) 860 nm peak for data shown in Fig. 5a, and (e) and (f) 683 and 860 nm peaks for data shown in Figs. 5b and c.

Changing the solvent to nonpolar toluene had major effects on the photochemical events. When ZnPc in the dyad was directly excited at 686 nm, peaks corresponding to the charge separated state were obvious (Fig. 5a). Two time constants, 916 and 1561 ps, likely due to two solution conformers, for CR were observed (Fig. 5d). Interestingly, when the dyad was excited at 466 nm corresponding to BPTI, SE signal corresponding to $^1\text{ZnPc}^*$ at 683 nm started emerging with signal saturation in less than 1 ps suggesting ultrafast energy transfer (Fig. 5b and e). At higher delay times, weak signal for the $\text{ZnPc}^+-\text{BPTI}^-$ state was observed in the 800-900 nm region (Fig. 5c). Time constant for CS was 80 ps while for CR two values of 100 and 455 ps were observed (Fig. 5f). These results indicate efficient excitation transfer, and although weak, formation of relatively long-lived charge separated state in toluene, especially from the directly excited $^1\text{ZnPc}^*$ state.

Conclusions

In summary, for the first time, BPTI has been covalently linked to ZnPc to create a new type of donor-acceptor dyad. Due to close distance and complementary absorption and emission spectral features, both ground- and excited state interactions were observed leading to excitation wavelength dependent, competitive excitation- and charge transfer events.

In polar solvent, electron transfer seems to prevail while in nonpolar solvent, excitation transfer was dominant. Due to close proximity, both charge separation and recombination processes were relatively rapid. Further efforts to synthesize donor-acceptor conjugates bearing BPTI to produce high-potential charge separated states with longer lifetimes, and external stimuli regulated charge separation, are underway in our laboratories.

This work has been supported by the Spanish Ministerio de Economía, Industria y Competitividad and the European FEDER funds (CTQ2016-77039-R AEI/FEDER, UE), and US-NSF (1401188 to FD).

Conflicts of interest

The authors declare no conflicts of interest.

Notes and references

^aÁrea de Química Orgánica, Instituto de Bioingeniería, Universidad Miguel Hernández, Avda. de la Universidad s/n 03202 Elche, Spain, E-mail: fdojdez@umh.es

^bDepartment of Chemistry, University of North Texas, 1155 Union Circle, #305070, Denton, TX 76203-5017, United States; E-mail: Francis.dsouza@unt.edu

^cDepartment of Physical Sciences and Mathematics, Wayne State College, 111 Main Street, Wayne, Nebraska 68787, USA

†Electronic Supplementary Information (ESI) available: [synthesis and experimental details, TCSPC decay curves, additional fs-TA spectral data]. See DOI: 10.1039/c000000x/

- D. Gust, T. A. Moore, A. L. Moore, *Acc. Chem. Res.* 2009, **42**, 1890; M. R. Wasielewski, *Acc. Chem. Res.* 2009, **42**, 1910; G. Bottari, G. de la Torre, D. M. Guldi, T. Torres, *Chem. Rev.* 2010, **110**, 6768; W. Leibl, P. Mathis, *Electron Transfer in Photosynthesis. Series on Photoconversion of Solar Energy*, 2004, **2**, 117; S. Lewis, D. G. Nocera, *Proc. Natl. Acad. Sci. U. S. A.* 2006, **103**, 15729; D. Kim, *Multiporphyrin Arrays: Fundamentals and Applications*, Pan Stanford Publishing, Singapore, 2012.
- G. de la Torre, C. G. Claessens and T. Torres, *Chem. Commun.*, 2007, 2000-2015; *Phthalocyanine Materials: Synthesis, Structure and Function*, ed. N. B. McKeown, Cambridge University Press, Cambridge, U.K., 1998; *Phthalocyanines-Properties and Applications Vol. 4*, ed. C. C. Lenhoff and A. B. P. Lever, VCH, Weinheim, Germany, 1996; *Phthalocyanines-Properties and Applications Vols. 2-3*, ed. C. C. Lenhoff and A. B. P. Lever, VCH, Weinheim, Germany, 1993; *Phthalocyanines-Properties and Applications Vol. 1*, ed. C. C. Lenhoff and A. B. P. Lever, VCH, Weinheim, Germany, 1989.
- R. Canton-Vitoria, H. B. Goebel, V. M. Blas-Ferrando, J. Ortiz, Y. Jang, F. Fernández-Lázaro, Á. Sastre-Santos, Y. Nakanishi, H. Shinohara, F. D'Souza and N. Tagmatarchis, *Angew. Chem., Int. Ed.*, 2019, **58**, 5712-5717; T. R. Kafle, B. Kattel, P. Yao, P. Zereshki, H. Zhao and W.-L. Chan, *J. Am. Chem. Soc.*, 2019, **141**, 11328-11336; E. Fazio, K. A. Winterfeld, A. López-Pérez, T. Torres, D. M. Guldi and G. de la Torre, *Nanoscale*, 2018, **10**, 22400-22408; M. Wolf, C. Villegas, O. Trukhina, J. L. Delgado, T. Torres, N. Martín, T. Clark and D. Guldi, *J. Am. Chem. Soc.*, 2017, **139**, 17474-17483; L. Martín-Gomis, F. Peralta-Ruiz, M. B. Thomas, F. Fernández-Lázaro, F. D'Souza and Á. Sastre-Santos, *Chem. Eur. J.*, 2017, **23**, 3863-3874; J. Arero, G. Kodis, R. A. Schmitz, D. D. Méndez-Hernández, T. A. Moore, A. L. Moore and D. Gust, *J. Porphyrins*

- Phthalocyanines*, 2015, **19**, 934-945; A. H. Al-Subi, A. Efimov, M. Niemi, N. V. Tkachenko and H. Lemmetyinen, *Chem. Phys. Lett.*, 2013, **572**, 96-100; G. Bottari, O. Trukhina, M. Ince and T. Torres, *Coord. Chem. Rev.*, 2012, **256**, 2453-2477.
- A. Nowak-Król and F. Würthner, *Org. Chem. Front.*, 2019, **6**, 1272-1318; A. Nowak-Król, K. Shoyama, M. Stolte and F. Würthner, *Chem. Commun.*, 2018, **54**, 13763-13772; F. Würthner, C. R. Saha-Möller, B. Fimmel, S. Ogi, P. Leowanawat and D. Schmidt, *Chem. Rev.*, 2016, **116**, 962-1052; F. Fernández-Lázaro, N. Zink-Lorre and Á. Sastre-Santos, *J. Mater. Chem. A*, 2016, **4**, 9336-9346; C. Li and H. Wonneberger, *Adv. Mater.*, 2012, **24**, 613-636; C. Huang, S. Barlow, S. R. Marder, *J. Org. Chem.*, 2011, **76**, 2386-2407; F. Würthner, *Chem. Commun.*, 2004, 1564-1579.
- B. Lü, Y. Chen, P. Li, B. Wang, K. Müllen and M. Yin, *Nature Commun.*, 2019, **10**, 767; J. M. Alzola, N. E. Powers-Riggs, N. T. La Porte, R. M. Young, T. J. Marks and M. R. Wasielewski, *J. Porphyrins Phthalocyanines*, 2019, DOI: 10.1142/S108842461950085819; P. W. Münich, C. Schierl, K. Dirian, M. Volland, S. Bauroth, L. Wibmer, Z. Syrgiannis, T. Clark, M. Prato and D. M. Guldi, *J. Am. Chem. Soc.*, 2018, **140**, 5427-5433; M. Koch, M. Myahkostupov, D. G. Oblinsky, S. Wang, S. Garakyaraghi, F. N. Castellano and G. D. Scholes, *J. Am. Chem. Soc.*, 2017, **139**, 5530-5537, **141**, 11328-11336.
- N. Zink-Lorre, E. Font-Sanchis, S. Seetharaman, P. A. Karr, Á. Sastre-Santos, F. D'Souza and F. Fernández-Lázaro, *Chem. Eur. J.*, 2019, **25**, 10123-10132; L. Martín-Gomis, F. Peralta-Ruiz, M. B. Thomas, F. Fernández-Lázaro, F. D'Souza and Á. Sastre-Santos, *Chem. Eur. J.*, 2017, **23**, 3863-3874.
- F. J. Céspedes-Guirao, L. Martín-Gomis, K. Ohkubo, S. Fukuzumi, F. Fernández-Lázaro and Á. Sastre-Santos, *Chem. Eur. J.*, 2011, **17**, 9153-9163.
- F. Follana-Berná, D. Inan, V. M. Blas-Ferrando, N. Gorczak, J. Ortiz, J. Manjón, F. Fernández-Lázaro, F. C. Grozema and Á. Sastre-Santos, *J. Phys. Chem. C*, 2016, **120**, 26508-26513.
- H. Langhals and S. Kirner, *Eur. J. Org. Chem.*, 2000, 365-380.
- H. Langhals and A. Hofer, *J. Org. Chem.*, 2013, **78**, 5889-5897; L. Flamigni, A. I. Ciuciu, H. Langhals, B. Böck and D. T. Gryko, *Chem. Asian J.*, 2012, **7**, 582-592; H. Langhals, B. Böck, T. Schmid and A. Marchuk, *Chem. Eur. J.*, 2012, **18**, 13188-13194; M. E. El-Khouly, M. Jaggi, B. Schmid, C. Blum, S.-X. Liu, S. Decurtins, K. Ohkubo and S. Fukuzumi, *J. Phys. Chem. C*, 2011, **115**, 8325-8334; H. Langhals, A. J. Esterbauer, A. Walter, E. Riedle and I. Pugliesi, *J. Am. Chem. Soc.*, 2010, **132**, 16777-16782; M. Jaggi, C. Blum, B. S. Marti, S.-X. Liu, S. Leutwyler and S. Decurtins, *Org. Lett.*, 2010, **12**, 1344-1347; H. Langhals, S. Poxleitner, O. Krotz, T. Pust and A. Walter, *Eur. J. Org. Chem.*, 2008, 4559-4562; S. Kalinin, M. Speckbacher, H. Langhals and B.-Å. Johansson, *Phys. Chem. Chem. Phys.*, 2001, **3**, 172-174; H. Langhals and M. Speckbacher, *Eur. J. Org. Chem.*, 2001, 2481-2485.
- S. Fukuzumi, K. Ohkubo, J. Ortiz, A. M. Gutiérrez, F. Fernández-Lázaro and Á. Sastre-Santos, *J. Phys. Chem. A*, 2008, **112**, 10744-10752.
- Gaussian 16*, Revision A.03, Gaussian, Inc., Wallingford, CT, 2016.
- H. C. Chen, C. P. Hsu, J. N. Reek, R. M. Williams and A. M. Brouwer, *ChemSusChem* 2015, **8**, 3639-3650.
- S. K. Das, A. Mahler, A. K. Wilson and F. D'Souza, *ChemPhysChem* 2014, **15**, 2462-2472.
- D. Rehm and A. Weller, *Isr. J. Chem.* 1970, **8**, 259-271.
- B. Ventura, H. Langhals, B. Bock and L. Flamigni, *Chem. Commun.* 2012, 48, 4226-4228; L. Flamigni, A. Zanelli, H. Langhals and B. Bock, *J. Phys. Chem. A* 2012, **16**, 1503-1509.

Table of Content

⁵ Zinc phthalocyanine - benzoperylenetriimide conjugate for solvent dependent ultrafast energy vs electron transfer[†]

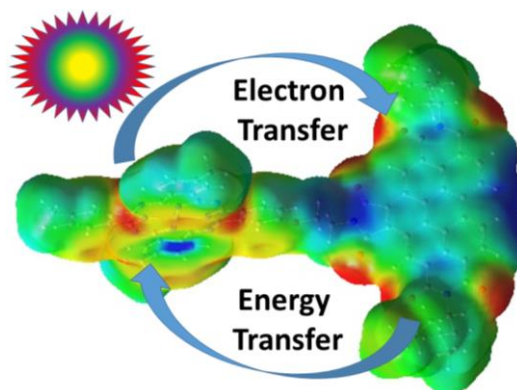
V. Navarro-Pérez,^a A. M. Gutiérrez-Vílchez,^a J. Ortiz,^a Á. Sastre-Santos,^a F. Fernández-Lázaro,^{*a} S. Seetharaman,^b M. J. Duffy,^c P. A. Karr,^c and F. D'Souza^{*b}

10

15

20

25



Ultrafast energy and electron transfer as a function of solvent polarity has been demonstrated using femtosecond transient absorption technique in a zinc phthalocyanine - benzoperylenetriimide conjugate.

30

35

40